The *bantam* Gene Regulates Drosophila Growth

David R. Hipfner, Katrin Weigmann and Stephen M. Cohen[1]

European Molecular Biology Laboratory, 69117 Heidelberg, Germany

Manuscript received February 12, 2002
Accepted for publication May 9, 2002

ABSTRACT

We report here the consequences of mutations of a novel locus, named *bantam*, whose product is involved in the regulation of growth in Drosophila. *bantam* mutant animals are smaller than wild type, due to a reduction in cell number but not cell size, and do not have significant disruptions in patterning. Conversely, overexpression of the *bantam* product using the EP element *EP(3)3622* causes overgrowth of wing and eye tissue. Overexpression in clones of cells results in an increased rate of cell proliferation and a matched increase in cellular growth rate, such that the resulting tissue is composed of more cells of a size comparable to wild type. These effects are strikingly similar to those associated with alterations in the activity of the cyclinD-cdk4 complex. However, epistasis and genetic interaction analyses indicate that *bantam* and cyclinD-cdk4 operate independently. Thus, the *bantam* locus represents a novel regulator of tissue growth.

MOST animals grow to a characteristic and reproducible size. Although the final size of the component parts of an animal can be greatly influenced by environmental factors such as nutrition, organ growth rates and size are also controlled by mechanisms intrinsic to the developing organs themselves (Bryant and Simpson 1984). The size of a given animal or organ is determined in large part by the number and size of its constituent cells. Consequently, the processes of cell division, cell death, and cell growth must be carefully regulated during development to ensure the correct and proportionate size of the adult animal (Conlon and Raff 1999).

The intrinsic and environmental mechanisms controlling growth have been the focus of considerable recent attention. Studies of the growth and development of Drosophila imaginal discs have begun to address the relative importance of cell growth and cell division in determining organ and body size (Edgar 1999; Lehner 1999; Oldham *et al.* 2000a; Stocker and Hafen 2000). Imaginal discs are the larval structures from which all adult epidermal structures of the fly are derived. These epithelial sacs arise as small clusters of 20–50 cells during embryogenesis (Cohen 1993). In the span of ~3 days during the larval instars, disc cells proliferate rapidly and increase in number ~1000-fold. As in higher organisms, imaginal disc cell divisions are regulated at G1-S and G2-M transitions. In addition, disc cell divisions are thought to be growth dependent, meaning that the cells normally do not divide until they have grown to a certain critical size or mass (Edgar and Lehner 1996). Experimental manipulation of cell division rates without corresponding changes in cell growth rates can have significant effects on cell size (Johnston *et al.* 1977; Weigmann *et al.* 1997; Neufeld *et al.* 1998). In Drosophila discs, accelerating the cell cycle by genetic means results in normal-sized discs with more and smaller cells. Conversely, slowing the cell cycle produces normal-sized discs with fewer and larger cells (Weigmann *et al.* 1997; Neufeld *et al.* 1998). The fact that final tissue size was unchanged in both cases, within limits, indicates that tissue growth is likely not regulated at the level of cell cycle control *per se*.

In contrast, a number of Drosophila genes have been identified that affect tissue growth directly. These genes all have in common the ability to regulate cellular growth rates. For example, genes encoding components of the insulin/phosphatidylinositol-3-kinase (PI3K) signaling pathway have been found to be instrumental in determining organ and body size. Overactivation of the pathway in imaginal discs causes tissue overgrowth by increasing the rate of cell growth. In the absence of a sufficient corresponding increase in the rate of cell division, this causes cells to divide at a larger than normal size (Goberdhan *et al.* 1999; Verdu *et al.* 1999; Weinkove *et al.* 1999; Gao *et al.* 2000). Conversely, decreased pathway activity reduces tissue growth by producing smaller cells (Böhni *et al.* 1999; Goberdhan *et al.* 1999; Montagne *et al.* 1999; Verdu *et al.* 1999; Weinkove *et al.* 1999; Gao *et al.* 2000), and in some cases also by reducing cell number (Böhni *et al.* 1999; Weinkove *et al.* 1999). The tumor-suppressor genes *TSC1* and *TSC2* restrict tissue growth by regulating cell growth rates via the insulin/PI3K pathway (Gao and Pan 2001; Potter *et al.* 2001; Tapon *et al.* 2001). In addition to components of the insulin/PI3K pathway, Drosophila homologs of *ras*, *myc*, and *TOR* have been

[1] *Corresponding author:* Developmental Biology Program, European Molecular Biology Laboratory, Meyerhofstrasse 1, 69117 Heidelberg, Germany. E-mail: cohen@embl-heidelberg.de

shown to promote cell growth (Johnston *et al.* 1999; Oldham *et al.* 2000b; Prober and Edgar 2000; Zhang *et al.* 2000).

In all of the foregoing examples the effects on tissue growth rates were mediated primarily by regulating cell growth rates. Consequently, the normal balance between the rate of cell growth and the rate of cell cycle progression was lost. Cells grew too fast and divided at abnormally large sizes. In contrast, the complex composed of Drosophila cyclin D (cycD) and cyclin-dependent kinase (cdk) 4 controls tissue growth in a manner that keeps the rates of cell growth and cell cycle progression in balance (Datar *et al.* 2000; Meyer *et al.* 2000). Tissue overgrowth due to overactivation of cycD-cdk4 results from an increase in the number of normal-sized cells. Mutation of cdk4 reduced tissue size by reducing cell number rather than cell size. Thus cycD-cdk4 appears to control the rate of growth by coordinated regulation of cell growth rates and cell cycle progression rates. With the exception of *ras*, both these classes of growth genes (those affecting primarily cell growth *vs.* those affecting cell growth and division rates) appear to be primarily involved in growth regulation, as they have minimal effects upon tissue patterning.

To identify additional genes involved in regulating imaginal disc growth, we performed a gain-of-function genetic screen using the EP method developed by Rorth (1996). When combined with a source of GAL4, the EP element will direct expression of genomic sequences adjacent to its site of insertion. Previous studies have shown that a high proportion of EP elements direct GAL4-dependent overexpression of endogenous genes (Rorth *et al.* 1998). We restricted our analysis to genes involved in growth by screening for EP elements that showed GAL4-dependent effects on tissue size without disrupting pattern. Here, we report the identification of a locus that we call *bantam* (*ban*), which influences tissue growth rates. We present evidence that *bantam* is involved in coordinately regulating cell growth and cell division to regulate the rate of normal tissue growth.

MATERIALS AND METHODS

Fly strains: The EP collection of 2300 lines (Rorth *et al.* 1998), as well as a new collection of 8500 independent strains carrying insertions of a modified EP element, termed EPg (Mata *et al.* 2000), were screened. The *sevenless* (*sev*), *optomotor blind*, *MS1096*, and *engrailed* (*en*) GAL4 drivers were used (Basler *et al.* 1989; Capdevila and Guerrero 1994; Fietz *et al.* 1995; Lecuit *et al.* 1996). EP lines were also screened for modifiers of the effects of overexpression of the tumor suppressor gene *expanded* (genotype: sev^{GAL4},*UAS-expanded*, svp^{AE127},ro^{1}/+; + *EP*; Boedigheimer and Laughon 1993; Blaumueller and Mlodzik 2000). ban^{L1170} is a *P*-element insertion allele, originally called *l(3)L1170*, and was obtained from the Bloomington Drosophila Stock Center. The *armadilloLacZ, FRT80B* stock was provided by Jessica Treisman. Other mutant and transgenic strains are described in the following references: *UAS-Dp110* (Leevers *et al.* 1996); *UAS-EGFP* (Denef *et al.* 2000); $UAS\text{-}GFP_{NLS}$ (Neufeld *et al.* 1998); *HS-FLP1* (Struhl and Basler 1993); *Actin5C > CD2 > GAL4* (Pignoni and Zipursky 1997); *UAS-cycD,UAS-cdk4* (Datar *et al.* 2000); and $cdk4^{3}$ (Meyer *et al.* 2000).

Mapping and characterization of *P*-element insertions in the *bantam* locus: Insertion sites of *EP(3)3622*, *EPg(3)30491*, and *EPg(3)35007* were determined by plasmid rescue according to standard procedures. Flanking sequences for ban^{L1170}, *EP(3)3208*, and *EP(3)3219* were available from the Berkeley Fly Database. These *P* elements are inserted in chromosome 3L at cytological position 61C7-8. They are clustered within 12.3 kb of one another in an interval of 42 kb containing no known or predicted genes. *EP(3)3622* contains two EP elements inserted in a back-to-back orientation at position 12,052 of genomic contig AE003469, with one basal promoter oriented proximally and one distally. The other *P* elements, with site of insertion in nucleotides relative to *EP(3)3622* (+, further distal; −, further proximal), are *EPg(3)35007* (−874); ban^{L1170} (−173); *EPg(3)30491* (−12); *EP(3)3208* (+2040); and *EP(3)3219* (+11,430). The ban^{L1170}, *EP(3)3208*, and *EP(3)3219* chromosomes are homozygous lethal, but in each case the lethality can be attributed to another locus on the chromosome. ban^{L1170}, *EP(3)3208*, and *EP(3)3219* are each viable *in trans* to the $ban^{\Delta 1}$ deletion. The revertant $ban^{L1170}R1$ chromosome, generated by excision of the ban^{L1170} *P* element, lost the *ban* mutant phenotype but remained homozygous lethal.

Generation and molecular characterization of the $ban^{\Delta 1}$ allele: To generate mutants for the *ban* locus, *P*-element excisions of *EP(3)3622* were generated. Excisions identified by the loss of the EP-element *mini-*w^{+} transgene were tested for complementation of the deletion *Df(3L)Ar11*, which removes from 61C3-4 to 61E. Excisions failing to complement this deficiency were analyzed by Southern blotting using genomic fragments derived from an *EP(3)3622* plasmid rescue construct. One excision causing early pupal lethality, $ban^{\Delta 1}$, was found to delete sequences both proximal and distal to the original EP insertion site. The ends of the $ban^{\Delta 1}$ deletion were mapped by genomic PCR on DNA from homozygous mutant third instar larvae with primer pairs spaced at 5- to 10-kb intervals along the chromosome. Once approximate limits of the breakpoint were identified, a 2.9-kb PCR product spanning the junction was amplified from the same genomic DNA and sequenced.

Analysis of adult phenotypes: All crosses for size comparison were conducted under identical, uncrowded conditions. Crosses with en^{GAL4} for Figure 3, C and D, were carried out at 29°. All other crosses were at 25°. For the *ban* complementation analysis, males heterozygous for the *P*-element insertion being tested and the $ban^{\Delta 1}$ allele were crossed to $ban^{\Delta 1}$/*TM2* females. In this way, each vial contained progeny of the tested genotype (*e.g.*, *P-element*/$ban^{\Delta 1}$) and $ban^{\Delta 1}$/*TM2* siblings. This allowed all measurements to be normalized relative to $ban^{\Delta 1}$/*TM2* sibling flies from within the same vial to eliminate the variability in adult body size resulting from differences in culture conditions between vials. Relative body mass was determined by weighing two or three sets of 20 male flies of each genotype from within a vial and taking the average. Final values in Table 1 are based on the average of at least two independent vials. Wing areas were measured using National Institutes of Health Image 1.59. To assess female fertility, virgin females (typically 40) of the appropriate genotype were crossed individually to wild-type males, and the number of viable adult offspring in each vial was counted ~20 days later. Scanning electron microscopy was performed as described (Blaumueller and Mlodzik 2000).

Imaginal disc growth analyses: For all larval analyses, larvae were staged essentially as described (Neufeld *et al.* 1998).

Embryos were collected for 3 hr. Twenty-four hours later, 65 newly hatched larvae of each genotype were transferred to fresh vials containing yeast paste. Discs from staged *en^{GAL4},UAS-EGFP/+* larvae [with or without *EP(3)3622*] were dissected at 112 ± 1.5 hr after egg laying (AEL) and fixed in 4% formaldehyde. Discs were stained with 4′,6-diamidino-2-phenylindole (DAPI) to visualize the nuclei and analyzed by confocal microscopy. The posterior compartment and total disc areas were measured from the green fluorescent protein (GFP) and blue (DAPI) channels, respectively, using the histogram function of Adobe Photoshop.

Flow cytometry: Flip-out clones were induced at 72 ± 1.5 hr AEL in staged larvae of the genotype *HS-FLP1/Act5C > CD2 > GAL4;UAS-GFP* [with or without *EP(3)3622* or *UAS-Dp110*] by heat shock at 38° for 1 hr. A total of 10–15 discs of each genotype were dissected in PBS at 112 ± 1.5 hr AEL, dissociated using trypsin, and stained with Hoechst 33342 as described (Neufeld *et al.* 1998). GFP content, cell cycle profiles, and forward scatter values were analyzed using a Cytomation MoFlo flow cytometer. Experiments were repeated three times with similar results.

Measurement of proliferation rates: Flip-out clones were induced at 72 ± 1.5 hr AEL in staged larvae of the genotype *HS-FLP1/Act5C > CD2 > GAL4;UAS-GFP$_{NLS}$* [with or without *EP(3)3622*] by heat shock at 37° for 15 min. Discs were dissected at 112 ± 1.5 hr AEL and fixed in 4% formaldehyde. GFP-positive cells within each clone were counted by epifluorescence microscopy. Cell doubling times were calculated using the formula $(\log 2/\log N)\,h$, where N is the average number of cells/clone and h is the hours between heat shock and dissection (Neufeld *et al.* 1998). The experiment was repeated twice with nearly identical results.

RESULTS

***bantam* mutants produce small flies with fertility defects:** In an overexpression screen for genes that affect tissue size, we identified several *P*-element insertions mapping within a 12.3-kb interval at cytological location 61C7-8 (Figure 1). *P*-element-mediated excision of *EP(3)3622* was used to produce a small deletion (Figure 1). The deletion is homozygous lethal at early pupal stages. Mutant larvae lack detectable imaginal discs. Flies heterozygous for the deletion and an independently isolated *P*-element insertion, *l(3)L1170*, are viable and normally patterned but are 15% smaller than sibling flies heterozygous for the deletion alone (Figure 2A, Table 1). The size reduction phenotype could be completely reverted by precise excision of the *l(3)L1170 P* element. Flies heterozygous for the deletion and a revertant of *l(3)L1170* (called *L1170 R1*) are comparable in size to siblings heterozygous for the deletion alone (Table 1), indicating that the *P*-element insertion disrupts a gene required for normal growth of the fly. We therefore named the locus *bantam*, to indicate that the mutants are smaller than normal.

We examined in more detail the adult phenotypes resulting from decreased *ban* function by testing other *P* elements mapping to the deleted region for complementation of the *ban$^{\Delta 1}$* excision allele. To eliminate the variability in adult body size resulting from differences in culture conditions between vials, measurements from flies heterozygous for *ban$^{\Delta 1}$* and the *P* element were always normalized to siblings heterozygous for *ban$^{\Delta 1}$* and the *TM2* balancer chromosome reared in the same vial. *EP(3)3622*, *EP(3)3208*, *EP(3)3219*, *EPg(3)30491*, and *EPg(3)35007* were each viable in combination with *ban$^{\Delta 1}$*. In addition to *l(3)L1170* (which we renamed *ban^{L1170}*), *EP(3)3622*, *EP(3)3208*, *EP(3)3219*, and *EPg(3)30491* caused a reduction in body size when *in trans* to *ban$^{\Delta 1}$*. In contrast, *EPg(3)35007* had no effect (Table 1). Although smaller, the *ban* mutant flies were normally proportioned and the majority did not show significant patterning defects, suggesting that the product of the *ban* locus is primarily involved in regulating growth of all adult structures.

Another characteristic affected by the *ban* mutations was female fertility. All allelic combinations with *ban$^{\Delta 1}$* that decreased adult size also caused a marked decrease in the average number of viable offspring produced by mutant females, whereas *EPg(3)35007* did not (not shown). For example, almost all *ban^{L1170}/ban$^{\Delta 1}$* females were sterile (2.5% fertile), in contrast to the 95% fertility rate of wild-type flies. As with the size reduction phenotype associated with *ban^{L1170}*, this effect on fertility could be completely reverted by precise excision of the *P* element, indicating that both phenotypes are due to the *ban^{L1170}* insertion.

We also analyzed flies homozygous for the viable *ban* alleles *EP(3)3622* and *EPg(3)30491*. In both cases, the homozygous flies showed the same reduced size and fertility defects as *EP/ban$^{\Delta 1}$ trans*-heterozygotes. Although the growth of *EP(3)3622* and *EPg(3)30491* homozygotes was affected to nearly the same extent as in the corresponding *EP/ban$^{\Delta 1}$* flies (Table 1), the fertility of homozygous females of both genotypes was less severely reduced [50% of females sterile for *EPg(3)30491/EPg(3)30491 vs.* 67.5% sterile for *EPg(3)30491/ban$^{\Delta 1}$*; 35% sterile for *EP(3)3622/EP(3)3622 vs.* 77.5% sterile for *EP(3)3622/ban$^{\Delta 1}$*; $n = 40$ in each case]. Neither *EP(3)3622* nor *EPg(3)30491* caused as great a reduction in adult size as *ban$^{\Delta 1}$* when *in trans* to the other *ban* *P*-element insertions (not shown). We conclude that both insertions are likely hypomorphic *ban* alleles.

Overexpression of *bantam* causes overgrowth: Several of the *ban* EP-element insertions were identified in an overexpression screen. Four EP insertions produced noticeable overexpression phenotypes [*EP(3)3622*, *EP(3)3208*, *EPg(3)30491*, and *EPg(3)35007*]. The more distally inserted *EP(3)3219* element did not. When expressed under the control of *en^{GAL4}*, *EP(3)3622* increased the size of the posterior compartment in wing imaginal discs (Figure 3A). Measurement of the relative areas of the posterior and anterior compartments of discs from *en^{GAL4}/+;EP(3)3622/+* larvae showed that a statistically significant increase of posterior to anterior area (P:A) ratio ($P < 0.001$; Figure 3B). To examine this phenotype in more detail we measured the effects of *EP(3)3622*, *EP(3)3208*, *EPg(3)30491*, and *EPg(3)35007* on growth in

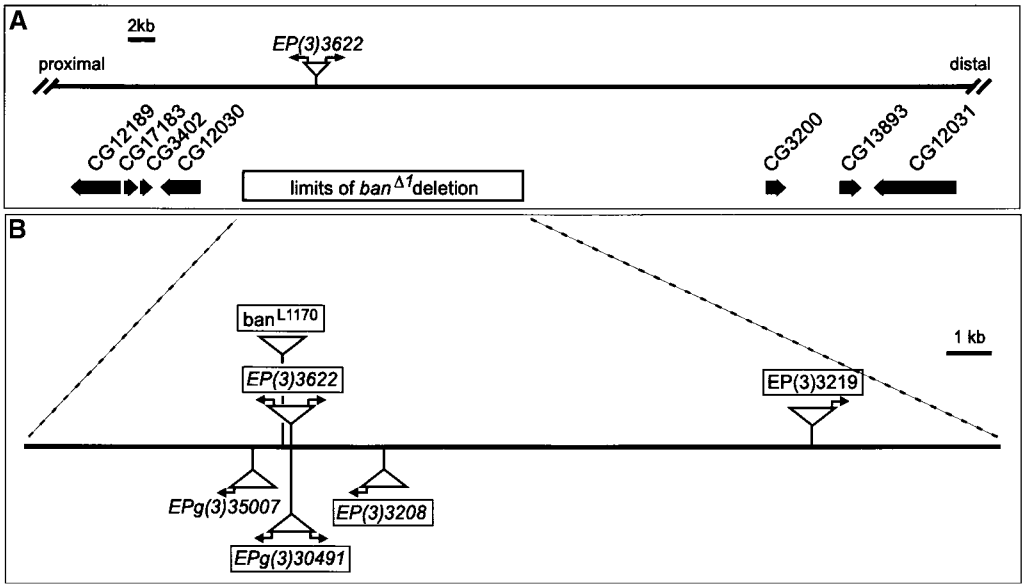

FIGURE 1.—Map of the *bantam* locus (61C7-8). (A) Map showing the positions of genes surrounding the *EP(3)3622* insertion site. Orientation and annotation numbers are indicated for several upstream and downstream genes. The region deleted in the $ban^{\Delta 1}$ allele is indicated below the map. (B) Magnification of the region deleted in the $ban^{\Delta 1}$ allele, showing the relative locations of *P* elements inserted in this interval. The orientation of the basal promoter is indicated by an arrow for each EP element. *EPg(3)30491* and *EP(3)3622* each contain two *P* elements inserted at the same position, oriented in opposite directions. EP elements producing a GAL4-dependent overexpression phenotype are indicated in italics. *P* elements producing a mutant phenotype *in trans* to $ban^{\Delta 1}$ are boxed.

the adult wing. Total wing area and the ratio of P:A compartment areas were measured. To exclude effects due to expression of en^{GAL4} in the region between veins 3 and 4 (BLAIR 1992), we used the area bounded by veins 1 and 3 as an estimate of anterior area and the area bounded by vein 4 and the posterior margin as an estimate of posterior area (illustrated in Figure 3D). en^{GAL4}-driven expression of *EPg(3)35007*, *EP(3)3208*, *EPg(3)30491*, and *EP(3)3622* caused statistically significant increases in the ratio of P:A areas compared to $en^{GAL4}/+$ wings ($P < 0.001$; Figure 3C). *EP(3)3622* had the strongest effect and was the only EP line to cause a statistically significant increase in the overall size of the wing (8%; $P < 0.001$; Figure 3C). Overgrowth of the posterior compartment occurred at the expense of the anterior compartment for the other EP lines, since there was no increase in overall wing size. This was also the case for *EP(3)3622*, because the magnitude of the increase in wing size was less than the relative increase in size of the posterior compartment. Only minor patterning abnormalities were observed in these wings (Figure 3D), suggesting that this EP element directs expression of a factor primarily involved in size regulation.

The effects of *EP(3)3622* overexpression are not limited to the wing. Expression of *EP(3)3622* in cells behind the morphogenetic furrow using the gmr^{GAL4} driver caused bulging of the eye (Figure 3E), suggesting extensive overgrowth. The eyes were also externally rough. *EP(3)3622* overexpression with appropriate drivers also caused duplication or triplication of interommatidial bristles in the eye and of macrochaete in the notum (data not shown). Similar effects on notum macrochaete have been described (ABDELILAH-SEYFRIED *et al.* 2000). These phenotypes are consistent with overproliferation of sensory organ precursor cells.

***bantam* mutant wings have fewer, but normal-sized, cells:** A number of mutants affecting growth of adult flies have been identified. Viable mutants of Drosophila *myc* and certain components of the insulin/PI3K signaling pathway have been shown to produce small, normally patterned adult flies. The decreased size of these animals is due in large part to a reduction in the size of cells in the adult (CHEN *et al.* 1996; BÖHNI *et al.* 1999; JOHNSTON *et al.* 1999; MONTAGNE *et al.* 1999). Flies lacking the product of the *cdk4* gene are also reduced in size. In this case, however, the size deficit is the result of a decrease in the number of adult cells, rather than of effects on cell size (MEYER *et al.* 2000). We analyzed wings from *ban* mutant flies to determine whether the growth deficit in these animals is due to decreased final adult cell size and/or cell number. Total wing areas were determined, and cell size was measured by number of wing hairs per unit area (each cell in the wing blade produces a single hair). Measurements for each allele *in trans* to $ban^{\Delta 1}$ were normalized to $ban^{\Delta 1}/TM2$ siblings. Wings from *ban* mutant flies were 9–13% smaller than $ban^{\Delta 1}/TM2$ siblings (Figure 2B, Table 1). For ban^{L1170}, *EP(3)3622*, and *EPg(3)30491* over $ban^{\Delta 1}$, the decrease in wing size was not due to a decrease in cell size. The number of hairs per unit area was not significantly different in these mutants *vs.* the corresponding control wings (Table 1). Instead, the decreased wing size was entirely attributable to a reduction in the number of cells in mutant wings by up to 12%.

The *EP(3)3219* insertion behaved differently, as the reduced wing size in $EP(3)3219/ban^{\Delta 1}$ was due primarily to a reduction in cell size rather than cell number. Interestingly, *EP(3)3219* had little or no effect on growth when combined with other *P*-element alleles [$EP(3)3219/ban^{L1170}$, 103% of sibling $ban^{\Delta 1}/TM2$ body mass; *EP(3)3219/EPg(3)*

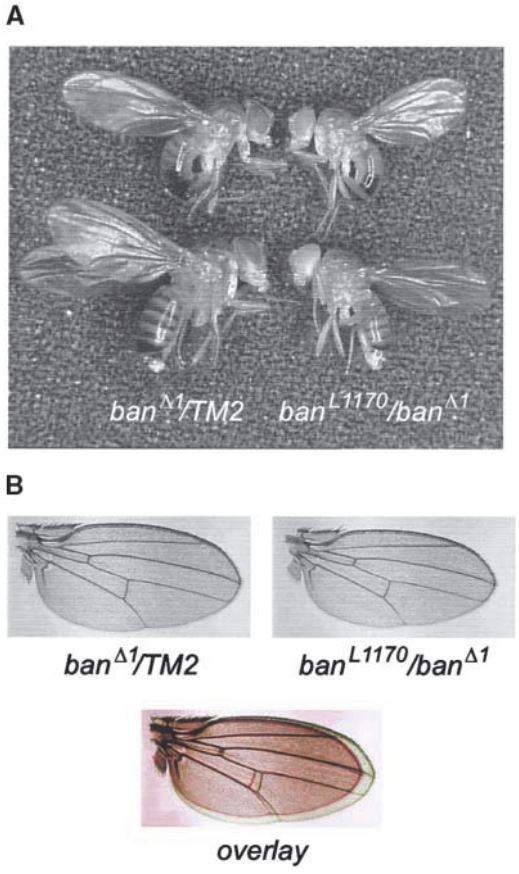

FIGURE 2.—*bantam* mutations reduce body and wing growth. (A) Comparison showing the reduced body size of $ban^{L1170}/ban^{\Delta 1}$ male and female flies compared to $ban^{\Delta 1}/TM2$ siblings. (B) Comparison of wing sizes from $ban^{L1170}/ban^{\Delta 1}$ and $ban^{\Delta 1}/TM2$ sibling flies. In the overlay the $ban^{L1170}/ban^{\Delta 1}$ wing is shown in red and the $ban^{\Delta 1}/TM2$ wing in green.

30491, 102%; *EP(3)3219/EP(3)3622*, 97%; averages from two independent vials]. These observations suggest that *EP(3)3219* affects a genetically separable locus and that it is not an allele of *ban*.

The cellular effects of *bantam* overexpression are distinct from the insulin signaling pathway: To examine how overexpression of *bantam* causes tissue overgrowth, we examined cell size and cell cycle profile in clones of *EP(3)3622*-expressing cells. *EP(3)3622*-expressing clones marked by coexpression of GFP or control GFP-expressing clones were induced at the end of second instar and allowed to grow until late third instar. Coexpression of GFP was used to identify and sort the *EP(3)3622*-expressing cells, which were directly compared for cell cycle phasing and cell sizes with GFP-negative wild-type control cells from the same disc. There was no apparent difference in the distribution of *EP(3)3622*-expressing and wild-type cells in the G1, S, and G2 phases of the cell cycle (Figure 4A). Cell size was compared using forward scatter values (NEUFELD *et al.* 1998). We observed a subtle difference between the EP-expressing and GFP-expressing control cells. Cells in control GFP-expressing clones were consistently slightly smaller than GFP-negative control cells (0.98; Figure 4B), whereas *EP(3)3622*-expressing, GFP-positive cells were consistently slightly larger (1.01; Figure 4C). Thus *EP(3)3622*-expressing cells were 3% larger than control GFP-expressing cells. Although reproducible, it is unclear whether this small difference is meaningful. For comparison, cells expressing the Dp110 catalytic subunit of PI3K, a known positive regulator of cellular growth rates, were 28% larger than control GFP-expressing cells, consistent with previous reports (WEINKOVE *et al.* 1999; Figure 4D). These results indicate that *EP(3)3622* expression has relatively little effect on cell size during the period of wing imaginal disc growth, consistent with the analysis of *ban* mutants.

These observations suggest that the mode of action of *ban* is distinct from Dp110 and other positive regulators of the insulin signaling pathway (WEINKOVE *et al.* 1999). Although *EP(3)3622* and Dp110 cause tissue overgrowth, they appear to have different effects at the cellular level. Activation of insulin signaling causes tissue growth by increasing the rate of cell growth more than the rate of cell division so that the overgrown tissue contains larger cells. *EP(3)3622* causes tissue overgrowth, but does not cause a comparable net increase in cell size. This suggested that *EP(3)3622*-induced tissue overgrowth is coupled with an increase in the rate of cell division such that the overgrown tissue contains more cells, as has been demonstrated for the cycD/cdk4 complex (DATAR *et al.* 2000). To test this we measured the cell-doubling rate by counting the average number of cells in clones allowed to grow for a defined time. Control GFP-expressing clones or *EP(3)3622*-expressing clones coexpressing GFP were induced in early third instar (72 hr AEL) and allowed to grow for 40 hr. The 187 control clones counted contained an average of 6.2 cells (median = 5), corresponding to a doubling time of 15.2 hr. In 213 clones expressing *EP(3)3622*, the average cell number was 7.0 (median = 7), corresponding to a doubling time of 14.2 hr. This difference is statistically significant ($P < 0.005$), and almost identical results were obtained in a second independent experiment. Together, these results indicate that *EP(3)3622*-overexpressing cells grow and divide more rapidly than control cells. Consistent with this observation, *EP(3)3622* causes a large increase in the number of cells in regions of the adult wing in which it has been expressed (not shown). These observations suggest that *ban* coordinately regulates the rates of cell growth and cell division.

***bantam* does not interact genetically with cyclinD/cdk4:** The growth and fertility phenotypes associated with gain and loss of *ban* function are similar to those associated with alterations in the activity of the cycD-cdk4 complex (DATAR *et al.* 2000; MEYER *et al.* 2000). Growth-impaired, viable mutants of both *ban* and *cdk4* are composed of a smaller number of wild-type-sized cells. In both cases, female fertility is strongly impaired.

TABLE 1

Phenotypic analysis of *bantam* heteroallelic mutants

Genotype	Viability (%) (*n*)[a]	Body mass (% control)[b]	Wing-blade area (10^6 μm^2)[c]	% control wing area	Cell area (μm^2)[d]	% control cell area	Intervein cell number[e]	% control cell number
ban$^{\Delta 1}$/+	—	105	—	—	—	—	—	—
ban$^{\Delta 1}$/*TM2*[f]	—	100	2.15–2.29	100	154–160	100	13,919–14,315	100
EPg(3)35007/ban$^{\Delta 1}$	100 (267)	103	—	—	—	—	—	—
ban^{L1170}*R1/ban*$^{\Delta 1}$	100 (267)	108	—	—	—	—	—	—
ban^{L1170}/*ban*$^{\Delta 1}$	80 (433)	85	1.88 ± 0.05[g]	87[g]	153 ± 4	99	12,298	88
EP(3)3622/ban$^{\Delta 1}$	100 (121)	78	2.08 ± 0.07[g]	91[g]	161 ± 8	101	12,914	90
EPg(3)30491/ban$^{\Delta 1}$	76 (243)	84	1.96 ± 0.06[g]	89[g]	152 ± 5	98	12,891	90
EP(3)3219/ban$^{\Delta 1}$	69 (216)	80	2.00 ± 0.07[g]	89[g]	146 ± 5[g]	92[g]	13,714	98
EP(3)3208/ban$^{\Delta 1}$	79 (207)	89	—	—	—	—	—	—
EP(3)3622/EP(3)3622	100 (97)	80	—	—	—	—	—	—
EPg(3)30491/EPg(3)30491	60 (211)	85	—	—	—	—	—	—

[a] Expressed as a percentage of expected number; n = number of flies scored.

[b] Obtained by weighing two to three sets of 20 males of each genotype/vial; values represent the average of at least two independent vials; values typically varied by <5% between vials.

[c] Based on measurements of 10 female wings of each genotype.

[d] Calculated by counting wing bristle density from 10 female wings in a 37,500-μm^2 rectangle between wing veins three and four, just distal to the anterior cross-vein, and converting to area/cell.

[e] Hypothetical number of intervein cells in one surface of the wing blade, obtained by dividing wing blade area/cell area.

[f] Measurements were taken separately for *ban*$^{\Delta 1}$/*TM2* flies from each vial, and these were used as control reference values (*i.e.*, 100%) within each vial; the range of values obtained is indicated.

[g] Significantly smaller than *ban*$^{\Delta 1}$/*TM2* siblings, $P < 0.001$.

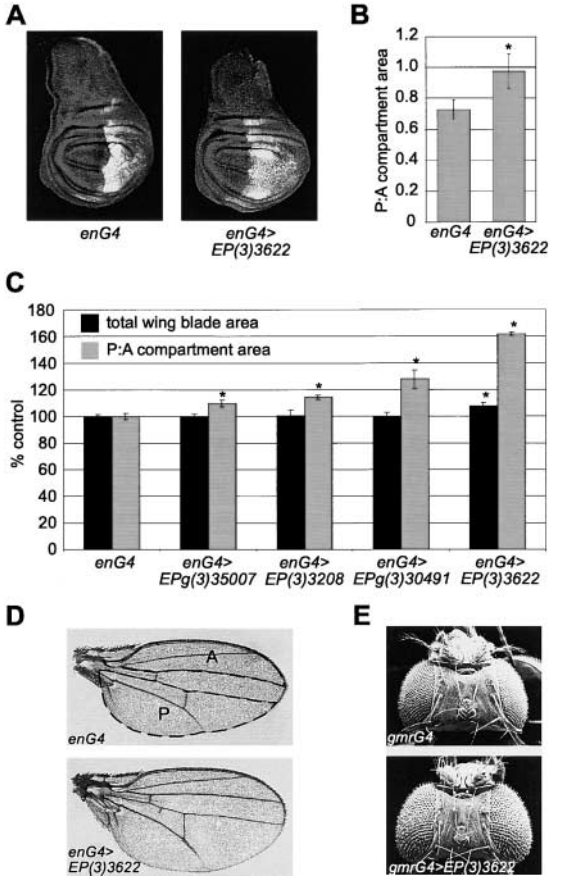

FIGURE 3.—EPs inserted in the *bantam* locus cause GAL4-dependent tissue overgrowth in the wing and eye. (A) Imaginal discs from staged larvae expressing EGFP with (right) or without (left) coexpression of *EP(3)3622* under the control of the en^{GAL4} driver were dissected at 112 hr AEL and fixed. Confocal images show discs with bright EGFP fluorescence marking the posterior compartment and less intense DAPI staining marking the entire disc (anterior is to the left). (B) Ratios of P:A compartment areas from en^{GAL4}/+ control and en^{GAL4}/+;*EP(3)3622*/+ discs ($n = 26$ for each genotype; *, significantly different from control; $P < 0.001$). (C) Quantitation of the ratio of P:A compartment sizes and total wing area. EPs were expressed in the posterior compartment of the wing using the en^{GAL4} driver. Anterior and posterior areas were measured from eight female wings of each genotype. Shaded bars: graph of average P:A wing-area ratios for flies expressing *EPg(3)35007*, *EP(3)3208*, *EPg(3)30491*, or *EP(3)3622* in the posterior compartment. Solid bars: graph of average total areas of the same set of wings. *, significantly different from *enG4*/+ controls ($P < 0.001$). (D) Comparison of en^{GAL4}/+ control and en^{GAL4}/+;*EP(3)3622*/+ wings. Anterior and posterior areas measured to calculate the P:A area ratios are outlined on the control wing. (E) Scanning electron microscopy images of heads from gmr^{GAL4}/+ control and gmr^{GAL4}/+;*EP(3)3622*/+ flies. *EP(3)3622* expression in the eye causes roughening and bulging, suggesting extensive overgrowth.

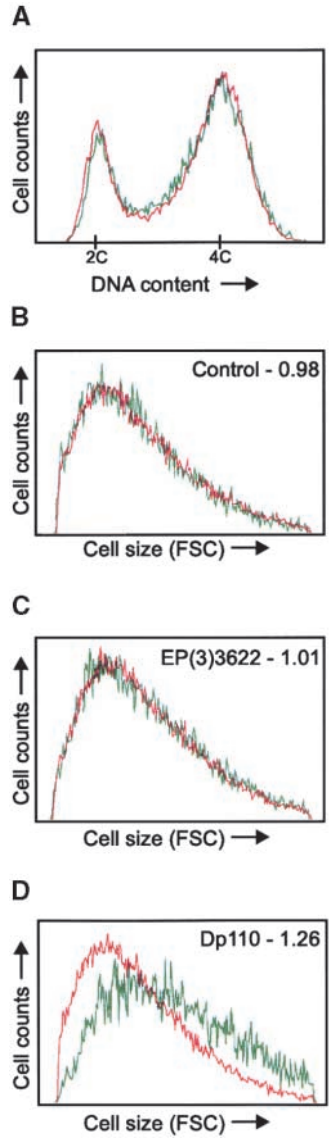

FIGURE 4.—*EP(3)3622* expression has little effect on disc cell size. Clones of cells expressing GFP alone or with either *EP(3)3622* or wild-type Dp110 were induced at 72 hr AEL. Discs were dissected at 112 hr AEL and cells were dissociated and analyzed by flow cytometry. In A–D, data for GFP and EP/transgene-expressing clonal cells and nonexpressing control cells from the same discs are in green and red, respectively. (A) Distribution of cells in G1 (2C DNA content), S (2C–4C), and G2 (4C) phases of the cell cycle for *EP(3)3622*-expressing and control cells. (B–D) Forward scatter analysis of cells from discs containing (B) control clones, (C) *EP(3)3622*-expressing clones, or (D) Dp110-expressing clones. Numbers represent the ratio of forward scatter values for GFP+/GFP− cells. Similar results were obtained in two additional independent experiments.

The characteristics of tissue growth driven by cycD-cdk4 and *ban* are indistinguishable. In proliferating epithelial cells of the wing imaginal disc, both increase rates of cell cycle progression and growth in a coordinated manner, so that cell size remains normal. Acceleration of the cell cycle is apparently uniform, as no alterations in cell cycle phasing are detected. In postmitotic cells in the eye, cycD-cdk4 coexpression led to cellular hypertrophy. The resulting bulging, overgrown eyes are very similar in appearance to eyes in which *ban* overexpression was driven with the same GAL4 driver (compare

Figure 3E with Figure 3G from Datar *et al.* 2000). These similarities raised the possibility that *ban* might act together with cycD-cdk4 to promote tissue growth. Consequently, we tested for genetic interactions between these growth regulators.

Importantly, both cycD and cdk4 are required to promote tissue growth. Expression of either alone is not sufficient (Datar *et al.* 2000). Therefore, to determine whether *ban*-driven overgrowth was dependent upon the activity of the cycD-cdk4 complex, we tested whether it could be blocked by removal of one of the components of this complex. We made use of the $MS1096^{GAL4}$ driver, which directs GAL4 expression in the dorsal compartment of the wing disc early in larval development and more broadly throughout the developing wing pouch later (Milán *et al.* 1998). Expression of *EP(3)3622* with $MS1096^{GAL4}$ resulted in significant overgrowth of the entire wing. The effect was greater in the dorsal compartment, such that the wings curved downwards (not shown). $MS1096^{GAL4}$/+;*EP(3)3622*/+ wings were 18% greater in area than control $MS1096^{GAL4}$/+ wings (Figure 5A). Overexpression of *ban* in a *cdk4* null mutant background ($cdk4^3/cdk4^3$) had no effect on the overgrowth phenotype. Wings of $MS1096^{GAL4}$/+;$cdk4^3/cdk4^3$;*EP(3)3622*/+ flies were 18% larger than those of $MS1096^{GAL4}$/+;$cdk4^3/cdk4^3$ flies (Figure 5A) and were also curved downward (not shown). As loss of *cdk4* had no apparent effect on *ban*-driven growth, we conclude that *ban* does not promote growth by regulating the activity of the cycD-cdk4 complex.

One of the main functions of cycD-cdk4 is believed to be suppression of the function of "pocket" proteins, such as pRb. However, genetic analyses in Drosophila suggested that the effects of cycD-cdk4 in promoting cellular growth are mediated at least in part by unknown downstream targets, independent of the fly pRb homolog RBF (Datar *et al.* 2000). We tested whether *ban* might be such a downstream target. Overexpression of cycD-cdk4 with the en^{GAL4} driver resulted in overgrowth of the posterior compartment of the wing, significantly increasing the P:A ratio by 11% (Figure 5B). This overgrowth was unaffected by halving the gene dosage of *ban* (Figure 5B). en^{GAL4}-driven cycD-cdk4 expression was also able to promote posterior compartment overgrowth to a comparable extent when the *ban* gene dosage was further reduced in the $ban^{L1170}/ban^{\Delta 1}$ allelic combination, although survival of these flies was poor (not shown). These observations suggest that the growth-promoting effects of cycD-cdk4 are not dependent upon *ban* levels.

To further evaluate the relationship between cycD-cdk4 and *ban*, we turned to an independent genetic assay for *ban* activity. Two of the *ban* EP insertions were identified initially in a genetic interaction screen as suppressors of the phenotype caused by overexpression of the *expanded* tumor suppressor gene. When misexpressed in the eye under the control of the sev^{GAL4} driver,

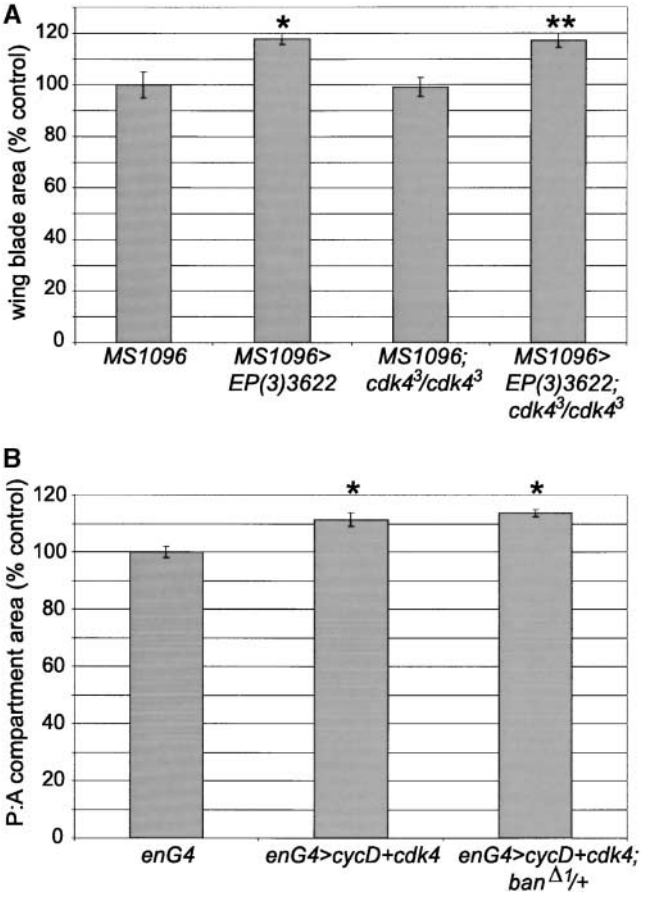

Figure 5.—*EP(3)3622* and cyclinD-cdk4 act independently to drive tissue growth. (A) Wing blade areas were measured from control flies and flies expressing *EP(3)3622* under the control of the $MS1096^{GAL4}$ driver in a wild-type or $cdk4^3$ mutant background. Seven female wings of each genotype were measured. Genotypes: $MS1096^{GAL4}$/+; $MS1096^{GAL4}$/+;*EP(3)3622*/+; $MS1096^{GAL4}$/+;$cdk4^3/cdk4^3$; and $MS1096^{GAL4}$/+;$cdk4^3/cdk4^3$;*EP(3)3622*/+. *, significantly different from $MS1096^{GAL4}$/+ ($P < 0.001$). **, significantly different from $MS1096^{GAL4}$/+;$cdk4^3/cdk4^3$ ($P < 0.001$). (B) CycD and cdk4 were coexpressed in the posterior compartment of the wing using the en^{GAL4} driver in a wild-type or $ban^{\Delta 1}$/+ background. Anterior and posterior areas were measured from six female wings of each genotype and expressed as P:A ratios. Genotypes: en^{GAL4}/+; en^{GAL4}/+;*UAS-cycD,UAS-cdk4*/+; and en^{GAL4}/+;*UAS-cycD,UAS-cdk4*/$ban^{\Delta 1}$. *, significantly different from en^{GAL4}/+ ($P < 0.001$).

expanded caused a reduction in eye size relative to wild type and external roughening and blistering (Figure 6, A and B; Blaumueller and Mlodzik 2000). Coexpression of *EP(3)3622* almost completely suppressed this phenotype, restoring the eye to nearly wild-type size and appearance (Figure 6C). Reducing *ban* function had the opposite effect. Introducing one copy of the $ban^{\Delta 1}$ allele noticeably reduced the overall eye size and increased the blistering in the central and anterior regions of the eye (Figure 6D). In contrast, alterations in cycD-cdk4 activity did not alter the *expanded* overexpression phenotype. Coexpression of cycD-cdk4 with *expanded* increased the overall size of the eye, consistent with

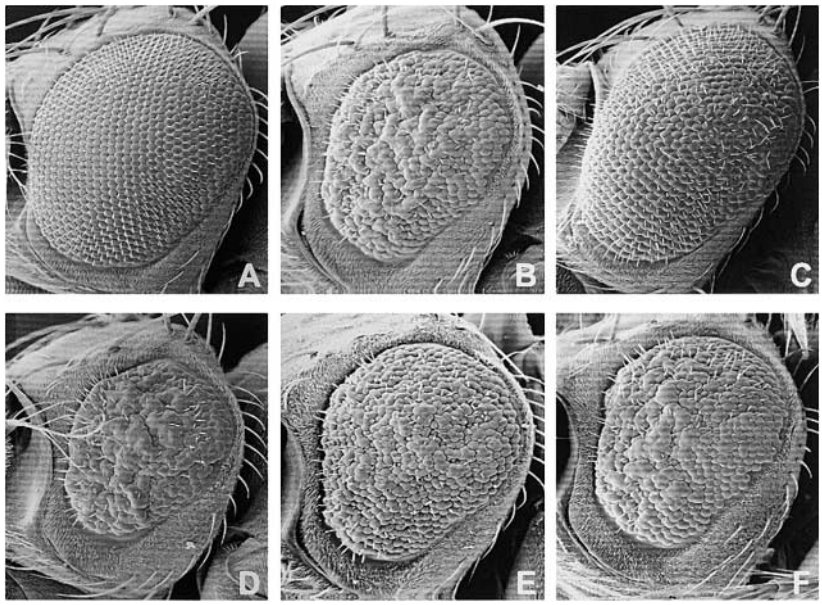

FIGURE 6.—*bantam*, but not cycD-cdk4, interacts genetically with the *expanded* tumor suppressor. Scanning electron microscopy images of eyes from female flies raised at 25°. Genotypes: (A) sev^{GAL4}/+. (B) sev^{GAL4},*UAS-expanded*, svp^{AE127},ro^{1}/+. (C) sev^{GAL4},*UAS-expanded*,svp^{AE127},ro^{1}/*EP(3)3622*. (D) sev^{GAL4},*UAS-expanded*,svp^{AE127},ro^{1}/$ban^{\Delta 1}$. (E) sev^{GAL4},*UAS-expanded*,svp^{AE127},ro^{1}/*UAS-cycD, UAScdk4*. (F) $cdk4^{3}$/+;sev^{GAL4},*UAS-expanded*, svp^{AE127},ro^{1}/+.

previous observations (DATAR *et al.* 2000), but had little effect on the roughness and blistering (Figure 6E). Removing one copy of *cdk4* had no effect (Figure 6F). The lack of a strong genetic interaction between *expanded* and cycD-cdk4 provides additional evidence that *bantam* is acting independently of this complex to promote coordinated cell growth and cell cycle progression.

Molecular characterization of the *bantam* locus: The $ban^{\Delta 1}$ deletion removes 21,147 nucleotides, extending from 5792 nucleotides proximal to 15,355 nucleotides distal to the *EP(3)3622* insertion site, and fails to complement the deficiency *Df(3L)Ar11* that removes from 61C3-4 to 61E. The $ban^{\Delta 1}$ deletion does not extend into the coding sequences of either of the two identified neighboring genes, *CG3200* (*Reg-2*) or the predicted *CG12030* (Figure 1). It is possible that noncoding or alternate exons of these genes might be located close to the EP elements. However, expression levels of *CG12030*, *Reg-2*, and *CG13893* (see Figure 1) were comparable in $ban^{\Delta 1}$ mutant and wild-type third instar larvae as assessed by Northern blot analysis (not shown). This suggests that the mutant phenotypes associated with $ban^{\Delta 1}$ are not due to effects on expression of any of these nearby genes. Similarly, we did not detect upregulation of *CG12030*, *Reg-2*, or *CG13893* or of the more distant genes *CG17181*, *CG12189*, or *CG12015* by *in situ* hybridization analysis of wing discs in which *EP(3)3622* was expressed.

It is possible that the *ban* locus may correspond to a gene contained at least in part within the ~41-kb interval between *CG12030* and *Reg-2*, which was not predicted in the CELERA/BDGP annotation. Although this intergenic region contains numerous short open reading frames, we have not found any meaningful homologies by BLAST sequence analysis. We have cloned two overexpressed transcription units mapping to this region that were first identified by *in situ* hybridization and Northern blot analysis of overexpression RNA with flanking genomic sequences as probes, or by RT-PCR using RNA from overexpressing larvae and an EP-element specific primer (RORTH 1996). However, neither of these transcripts is able to reproduce the overgrowth phenotype when expressed from a transgene (not shown). A more complete understanding of the mechanism of *ban* action will await molecular characterization of the gene product.

DISCUSSION

***bantam* is required for normal tissue growth:** *ban* gene function appears to be important for regulation of tissue growth rates. Several EP elements inserted in this locus, most notably *EP(3)3622*, are capable of promoting substantial tissue overgrowth in the eye and wing in a GAL4-dependent manner. Conversely, *ban* mutations decrease tissue growth. Mutant phenotypes range from decreased body size to lethality. The strongest available allele is a small deletion that does not remove any known genes. This allele is pupal lethal and causes the absence of detectable imaginal discs. The simplest explanation for the reciprocal nature of gain-of-function and loss-of-function phenotypes is that *EP(3)3622* is driving expression of the same transcription unit that is affected by *ban* mutations. This is further supported by the specific and reciprocal nature of the genetic interaction of gain and loss of *ban* function with the *expanded* tumor suppressor gene in the eye. However, this remains to be confirmed by molecular characterization of the locus. Growth regulation appears to be a primary function of *ban*, as *EP(3)3622* expression does not cause significant patterning alterations, and *ban* mutant flies, although small, are proportioned normally.

***bantam* coordinates cell growth and division rates to regulate tissue growth:** Our results suggest that *ban* regulates tissue growth by a mechanism that involves coordinated stimulation of cell growth and cell division. *ban* alters tissue growth through effects on cell number rather than cell size. Decreased *ban* function causes a reduction in cell number in the adult wing, but the surviving cells are of wild-type size, suggesting a coordinated decrease in the rate of cell growth and division. Activation of *EP(3)3622* has the opposite effect on cell number, causing an increase in the rate at which imaginal disc cells proliferate. Despite this increased proliferation rate, cell sizes are little changed. These observations suggest that the rate of increase in cell division is coordinated with the rate of increase of cell mass when *ban* is overexpressed. The effects of *ban* on growth and fertility are remarkably similar to those of cycD-cdk4. However, we have found no evidence of a direct connection between cycD-cdk4 and *ban*. It seems unlikely that *ban* regulates growth by controlling the activity of cycD-cdk4, because *ban*-driven overgrowth is unaffected in the absence of cdk4. Similarly, cycD-cdk4-driven growth is unaffected by reduction of *ban*, indicating that *ban* is unlikely to be a downstream effector. We favor the view that *ban* and cycD-cdk4 act independently. The similarity in their growth phenotypes suggests that they may have some targets in common. However, as attested to by the differences in their interactions with *expanded*, they clearly can act differently as well.

Growth and pattern formation: The imaginal discs are patterned while they grow. The secreted signaling proteins Decapentaplegic (Dpp) and Wingless pattern the wing and leg discs along their main axes. Dpp and Wingless signaling are also required in some way for disc growth. The parts of the discs that produce the appendages are very small in flies lacking either signal (Spencer *et al.* 1982; Diaz-Benjumea *et al.* 1994; Zecca *et al.* 1995; Neumann and Cohen 1996). Cells unable to transduce the Dpp or Wingless signals display cell-autonomous defects in proliferation and are lost from the disc (Peifer *et al.* 1991; Burke and Basler 1996). To date it has not been reported whether loss of cells under these conditions is due to reduced proliferation or to reduced survival. However, recent studies suggest that Dpp signaling may directly influence cell proliferation in the wing disc (Martin-Castellanos and Edgar 2002). Wingless signaling has been shown in one situation to repress growth at late stages of wing development, in part by negative regulation of *dmyc* expression (Johnston and Edgar 1998; Johnston *et al.* 1999). If Dpp and Wingless act directly to regulate tissue growth, we would expect them to coordinately regulate cell growth and cell division rates. It will be of interest to learn whether *ban* and/or cycD-cdk4 mediate the growth effects of these signaling molecules.

Compartments and imaginal discs as units of size control: Altering cell division rates does not alter compartment size, but can increase or decrease the number of cells per compartment (Weigmann *et al.* 1997; Neufeld *et al.* 1998). This is consistent with the effects of Minute mutations that vary the proportion of a compartment that can be contributed by the progeny of a single cell, without affecting compartment size or shape (Morata and Ripoll 1975). However, as first shown by Leevers *et al.* (1996), it is possible to alter the size of one compartment relative to another by manipulating activity of the insulin/PI3K pathway (Leevers *et al.* 1996). PI3K-induced overgrowth requires that the pathway be activated in all cells of the compartment. Clones of overgrowing cells do not affect the size of the compartment (Teleman and Cohen 2000). Thus a mechanism must exist that allows a population of cells to measure the size of the compartment. Interestingly, it has been found that altering the size of the compartment feeds back by an unknown mechanism to alter the shape of the Dpp morphogen gradient (Teleman and Cohen 2000).

Overexpression of *ban* with en^{GAL4} promoted significant overgrowth of the posterior compartment. We noted that posterior compartment overgrowth was compensated for by a nonautonomous reduction in the final size of the anterior compartment in most cases. This compensation suggests that total disc size may also be regulated to some extent during development. Only in the case of the strongest EP element, *EP(3)3622*, were total disc and wing size increased.

These observations suggest that there may be multiple layers of size control operating during imaginal disc development. Morphogen gradients influence tissue growth. Tissue growth rates influence compartment size and morphogen gradient shape. Finally, size compensation mechanisms exist to control both compartment and disc size. At present, little is known about the size-sensing mechanisms, except that we can override them by stimulating cell and tissue growth rates by various experimental means. Identifying how size is measured during tissue growth poses a significant challenge.

We thank Ann Atzberger for flow cytometric analyses, Ann Mari Voie for preparing transgenic fly strains, and Christine Blaumueller for fly stocks and advice; Enrique Martin-Blanco for sharing information on the *EP(3)3622* insertions prior to publication; and Pernille Rørth and members of the lab for helpful discussions. K.W. and D.R.H. were fellows of the European Molecular Biology Organization. D.R.H. was a fellow of the Human Frontiers Science Program Organization.

LITERATURE CITED

Abdelilah-Seyfried, S., Y. M. Chan, C. Zeng, N. J. Justice, S. Younger-Shepherd *et al.*, 2000 A gain-of-function screen for genes that affect the development of the Drosophila adult external sensory organ. Genetics **155:** 733–752.

Basler, K., P. Siegrist and E. Hafen, 1989 The spatial and temporal expression pattern of *sevenless* is exclusively controlled by gene-internal elements. EMBO J. **8:** 2381–2386.

Blair, S., 1992 *engrailed* expression in the anterior lineage compart-

ment of the developing wing blade of Drosophila. Development **115:** 21–33.

Blaumueller, C. M., and M. Mlodzik, 2000 The Drosophila tumor suppressor *expanded* regulates growth, apoptosis, and patterning during development. Mech. Dev. **92:** 251–262.

Boedigheimer, M., and A. Laughon, 1993 *Expanded*: a gene involved in the control of cell proliferation in imaginal discs. Development **118:** 1291–1301.

Böhni, R., J. Riesgo-Escovar, S. Oldham, W. Brogiolo, H. Stocker *et al.*, 1999 Autonomous control of cell and organ size by CHICO, a Drosophila homolog of vertebrate IRS1-4. Cell **97:** 865–875.

Bryant, P. J., and P. Simpson, 1984 Intrinsic and extrinsic control of growth in developing organs. Q. Rev. Biol. **59:** 387–415.

Burke, R., and K. Basler, 1996 Dpp receptors are autonomously required for cell proliferation in the entire developing Drosophila wing. Development **122:** 2261–2269.

Capdevila, J., and I. Guerrero, 1994 Targeted expression of the signalling molecule decapentaplegic induces pattern duplications and growth alterations in Drosophila wings. EMBO J. **13:** 4459–4468.

Chen, C., J. Jack and R. S. Garofalo, 1996 The Drosophila insulin receptor is required for normal growth. Endocrinology **137:** 846–856.

Cohen, S. M., 1993 Imaginal disc development, pp. 747–841 in *Drosophila Development*, edited by A. Martinez-Arias and M. Bate. Cold Spring Harbor Laboratory Press, Cold Spring Harbor, NY.

Conlon, I., and M. Raff, 1999 Size control in animal development. Cell **96:** 235–244.

Datar, S. A., H. W. Jacobs, A. F. de La Cruz, C. F. Lehner and B. A. Edgar, 2000 The Drosophila cyclin D-cdk4 complex promotes cellular growth. EMBO J. **19:** 4543–4554.

Denef, N., D. Neubueser, L. Perez and S. M. Cohen, 2000 Hedgehog induces opposite changes in turnover and subcellular localization of Patched and Smoothened. Cell **102:** 521–531.

Diaz-Benjumea, F. J., B. Cohen and S. M. Cohen, 1994 Cell interactions between compartments establishes the proximal-distal axis of Drosophila limbs. Nature **372:** 175–179.

Edgar, B. A., 1999 From small flies come big discoveries about size control. Nat. Cell Biol. **1:** E191–193.

Edgar, B. A., and C. F. Lehner, 1996 Developmental control of cell cycle regulators: a fly's perspective. Science **274:** 1646–1652.

Fietz, M. J., A. Jacinto, A. M. Taylor, C. Alexandre and P. W. Ingham, 1995 Secretion of the amino-terminal fragment of Hedgehog protein is necessary and sufficient for *hedgehog* signalling in Drosophila. Curr. Biol. **5:** 643–650.

Gao, X., and D. Pan, 2001 *TSC1* and *TSC2* tumor suppressors antagonize insulin signaling in cell growth. Genes Dev. **15:** 1383–1392.

Gao, X., T. P. Neufeld and D. Pan, 2000 Drosophila *PTEN* regulates cell growth and proliferation through PI3K-dependent and -independent pathways. Dev. Biol. **221:** 404–418.

Goberdhan, D. C., N. Paricio, E. C. Goodman, M. Mlodzik and C. Wilson, 1999 Drosophila tumor suppressor *PTEN* controls cell size and number by antagonizing the Chico/PI3-kinase signaling pathway. Genes Dev. **13:** 3244–3258.

Johnston, G. C., J. R. Pringle and L. H. Hartwell, 1977 Coordination of growth with cell division in the yeast *Saccharomyces cerevisiae*. Exp. Cell Res. **105:** 79–98.

Johnston, L. A., and B. A. Edgar, 1998 Wingless and Notch regulate cell-cycle arrest in the developing Drosophila wing. Nature **394:** 82–84.

Johnston, L. A., D. A. Prober, B. A. Edgar, R. N. Eisenman and P. Gallant, 1999 Drosophila myc regulates cellular growth during development. Cell **98:** 779–790.

Lecuit, T., W. J. Brook, M. Ng, M. Calleja, H. Sun *et al.*, 1996 Two distinct mechanisms for long-range patterning by Decapentaplegic in the Drosophila wing. Nature **381:** 387–393.

Leevers, S. J., D. Weinkove, L. K. MacDougall, E. Hafen and M. D. Waterfield, 1996 The Drosophila phosphoinositide 3-kinase Dp110 promotes cell growth. EMBO J. **15:** 6584–6594.

Lehner, C. F., 1999 The beauty of small flies. Nat. Cell Biol. **1:** E129–130.

Martin-Castellanos, C., and B. A. Edgar, 2002 A characterization of the effects of Dpp signaling on cell growth and proliferation in the Drosophila wing. Development **129:** 1003–1013.

Mata, J., S. Curado, A. Ephrussi and P. Rorth, 2000 Tribbles coordinates mitosis and morphogenesis in Drosophila by regulating string/CDC25 proteolysis. Cell **101:** 511–522.

Meyer, C. A., H. W. Jacobs, S. A. Datar, W. Du, B. A. Edgar *et al.*, 2000 Drosophila cdk4 is required for normal growth and is dispensable for cell cycle progression. EMBO J. **19:** 4533–4542.

Milán, M., F. Diaz-Benjumea and S. M. Cohen, 1998 *Beadex* encodes an LMO protein that regulates Apterous LIM-homeodomain activity in Drosophila wing development: a model for LMO oncogene function. Genes Dev. **12:** 2912–2920.

Montagne, J., M. J. Stewart, H. Stocker, E. Hafen, S. C. Kozma *et al.*, 1999 Drosophila S6 kinase: a regulator of cell size. Science **285:** 2126–2129.

Morata, G., and P. Ripoll, 1975 Minutes: mutants of Drosophila autonomously affecting cell division rate. Dev. Biol. **42:** 211–221.

Neufeld, T. P., A. F. de la Cruz, L. A. Johnston and B. A. Edgar, 1998 Coordination of growth and cell division in the Drosophila wing. Cell **93:** 1183–1193.

Neumann, C. J., and S. M. Cohen, 1996 Distinct mitogenic and cell fate specification functions of *wingless* in different regions of the wing. Development **122:** 1781–1789.

Oldham, S., R. Bohni, H. Stocker, W. Brogiolo and E. Hafen, 2000a Genetic control of size in Drosophila. Philos. Trans. R. Soc. Lond. B Biol. Sci. **355:** 945–952.

Oldham, S., J. Montagne, T. Radimerski, G. Thomas and E. Hafen, 2000b Genetic and biochemical characterization of dTOR, the Drosophila homolog of the target of rapamycin. Genes Dev. **14:** 2689–2694.

Peifer, M., C. Rauskolb, M. Williams, B. Riggleman and E. Wieschaus, 1991 The segment polarity gene *armadillo* interacts with the *wingless* signaling pathway in both embryonic and adult pattern formation. Development **111:** 1029–1043.

Pignoni, F., and S. L. Zipursky, 1997 Induction of Drosophila eye development by *decapentaplegic*. Development **124:** 271–278.

Potter, C. J., H. Huang and T. Xu, 2001 Drosophila Tsc1 functions with Tsc2 to antagonize insulin signaling in regulating cell growth, cell proliferation, and organ size. Cell **105:** 357–368.

Prober, D. A., and B. A. Edgar, 2000 Ras1 promotes cellular growth in the Drosophila wing. Cell **100:** 435–446.

Rorth, P., 1996 A modular misexpression screen in Drosophila detecting tissue specific phenotypes. Proc. Natl. Acad. Sci. USA **93:** 12418–12422.

Rorth, P., K. Szabo, A. Bailey, T. Laverty, J. Rehm *et al.*, 1998 Systematic gain-of-function genetics in Drosophila. Development **125:** 1049–1057.

Spencer, F., M. Hoffman and W. M. Gelbart, 1982 Decapentaplegic: a gene complex affecting morphogenesis in *Drosophila melanogaster*. Cell **28:** 451–461.

Stocker, H., and E. Hafen, 2000 Genetic control of cell size. Curr. Opin. Genet. Dev. **10:** 529–535.

Struhl, G., and K. Basler, 1993 Organizing activity of *wingless* protein in Drosophila. Cell **72:** 527–540.

Tapon, N., N. Ito, B. J. Dickson, J. E. Treisman and I. K. Hariharan, 2001 The Drosophila tuberous sclerosis complex gene homologs restrict cell growth and cell proliferation. Cell **105:** 345–355.

Teleman, A. A., and S. M. Cohen, 2000 Dpp gradient formation in the Drosophila wing imaginal disc. Cell **103:** 971–980.

Verdu, J., M. A. Buratovich, E. L. Wilder and M. J. Birnbaum, 1999 Cell-autonomous regulation of cell and organ growth in Drosophila by Akt/PKB. Nat. Cell Biol. **1:** 500–506.

Weigmann, K., S. M. Cohen and C. Lehner, 1997 Cell cycle progression, growth and patterning in imaginal discs despite inhibition of cell division after inactivation of Drosophila Cdc2 kinase. Development **124:** 3555–3563.

Weinkove, D., T. P. Neufeld, T. Twardzik, M. D. Waterfield and S. J. Leevers, 1999 Regulation of imaginal disc cell size, cell number and organ size by Drosophila class I(A) phosphoinositide 3-kinase and its adaptor. Curr. Biol. **9:** 1019–1029.

Zecca, M., K. Basler and G. Struhl, 1995 Sequential organizing activities of *engrailed, hedgehog* and *decapentaplegic* in the Drosophila wing. Development **121:** 2265–2278.

Zhang, H., J. P. Stallock, J. C. Ng, C. Reinhard and T. P. Neufeld, 2000 Regulation of cellular growth by the Drosophila target of rapamycin dTOR. Genes Dev. **14:** 2712–2724.

Communicating editor: T. Schüpbach